

Subgraph-Aware Training of Text-based Methods for Knowledge Graph Completion

Youmin Ko*, Hyemin Yang*, Taeuk Kim, Hyunjoon Kim[†]

Hanyang University

{youminkk021, hmym7308, kimtaeuk, hyunjoonkim}@hanyang.ac.kr

Abstract

Fine-tuning pre-trained language models (PLMs) has recently shown a potential to improve knowledge graph completion (KGC). However, most PLM-based methods encode only textual information, neglecting various topological structures of knowledge graphs (KGs). In this paper, we empirically validate the significant relations between the structural properties of KGs and the performance of the PLM-based methods. To leverage the structural knowledge, we propose a Subgraph-Aware Training framework for KGC (SATKGC) that combines (i) subgraph-aware mini-batching to encourage hard negative sampling, and (ii) a new contrastive learning method to focus more on harder entities and harder negative triples in terms of the structural properties. To the best of our knowledge, this is the first study to comprehensively incorporate the structural inductive bias of the subgraphs into fine-tuning PLMs. Extensive experiments on four KGC benchmarks demonstrate the superiority of SATKGC. Our code is available.

1 Introduction

Factual sentences, e.g., Leonardo da Vinci painted Mona Lisa, can be represented as *entities*, and *relations* between the entities. Knowledge graphs treat the entities (e.g., Leonardo da Vinci and Mona Lisa) as nodes, and the relations (e.g., painted) as edges. Each edge and its endpoints are denoted as a triple (h, r, t) where h, r and t are a head entity, a relation, and a tail entity respectively. Since KGs can represent complex relations between entities, they serve as key components for knowledge-intensive applications (Ji et al., 2021; Xiong et al., 2017; He et al., 2017; Zhang et al., 2016; Liu et al., 2021).

Despite their applicability, real-world KGs miss factual relations, which can be inferred from existing facts in the KGs. Hence, the task of knowledge

graph completion (KGC) has become an active research topic (Ji et al., 2021). Given an incomplete triple $(h, r, ?)$, this task is to predict the correct tail t . A true triple (h, r, t) in KG and a false triple (h, r, \hat{t}) which does not exist in KG are called positive and negative, respectively. A negative triple difficult for a KGC method to distinguish from its corresponding positive triple is regarded as a hard negative triple.

Existing KGC methods are categorized into two approaches. An embedding-based approach learns embeddings of entities in continuous vector spaces, but ignores contextualized text information in KGs, thus being inapplicable to entities and relations unseen in training (Bordes et al., 2013; Balazevic et al., 2019). A text-based approach, based on pretrained language models (PLMs), learns textual representations of KGs, but suffers from a lack of structural knowledge in KGs (Wang et al., 2022a).

Meanwhile, contrastive learning has become a key component of representation learning (Kalanidis et al., 2020; Robinson et al., 2021; Gao et al., 2021; Wang et al., 2022b), but an important aspect of contrastive learning, i.e., the effect of hard negatives, has so far been underexplored in KGC. In this paper, we empirically validate significant relationships between the structural properties of KGs and the performance of the PLM-based KGC methods.

To address the aforementioned longstanding limitations of two KGC approaches by utilizing the above relationships, we hypothesize that incorporating the structural inductive bias of KGs into both sampling hard negatives and fine-tuning PLMs leads to a major breakthrough in learning comprehensive representations of KGs. To this end, we propose a Subgraph-Aware Training framework for KGC (SATKGC), which (i) samples subgraphs of a KG to treat triples of each subgraph as a mini-batch to encourage hard negative sampling, and (ii) fine-tunes a PLM via contrastive learning which focuses

*Equal contribution.

[†]Corresponding author.

more on structurally harder entities and structurally harder negative triples induced by topological bias in the KG. To sum up, we make four contributions.

- We provide key insights that the topological structure of KGs is closely related to the performance of PLM-based KGC methods.
- We propose a subgraph-aware training strategy for PLM-based KGC methods, which is effective in sampling in-batch hard negatives.
- We propose a novel contrastive learning method that gives different importances to positive and negative triples based on the structural properties of KGs.
- We conduct extensive experiments on four KGC benchmarks to demonstrate the superiority of SATKGC over existing KGC methods.

2 Related Work

An **embedding-based approach** maps complex and structured knowledge into low-dimensional spaces. This approach computes the plausibility of a triple using translational scoring functions on the embeddings of the triple’s head, relation, and tail (Bordes et al., 2013; Sun et al., 2019; Zhang et al., 2022; Ge et al., 2023), e.g., $h + r \approx t$, or semantic matching functions which match latent semantics of entities and relations (Nickel et al., 2011; Yang et al., 2015; Trouillon et al., 2016; Balazevic et al., 2019). This approach exploits the spatial relations of the embeddings, but cannot make use of texts in KGs, i.e., the source of semantic relations.

In contrast, a **text-based approach** learns contextualized representations of the textual contents (e.g., names and descriptions) of entities and relations by leveraging PLMs (Yao et al., 2019; Wang et al., 2021b; Xie et al., 2016; Daza et al., 2021; Kim et al., 2020; Wang et al., 2022a; Chen et al., 2022; Zhang et al., 2023a). More recently, there has been a significant increase in the adoption of large language models (LLMs) in KGC (Zhang et al., 2023c). However, these PLM-based models are often oblivious to structural inductive bias in KGs.

A few attempts have been made to utilize the above two approaches at once. StAR (Wang et al., 2021d) proposes an ensemble model incorporating an output of a Transformer encoder (Vaswani et al., 2017) with a triple score produced by RotatE (Sun et al., 2019). CSProm-KG (Chen et al., 2023) trains KG embeddings through the soft prompt for

a PLM. Nevertheless, the integration of structural and textual information in a KG in training has not yet been fully realized.

Contrastive learning, shown to be effective in various fields (Wu et al., 2018; Haque et al., 2022; Fang et al., 2020; Zhang et al., 2023b; Gao et al., 2021), has recently emerged as a promising approach in the context of KGC (Wang et al., 2022a; Yang et al., 2020; Qiao et al., 2023). Despite a critical aspect of contrastive learning, the effect of hard negatives has been overlooked in KGC.

Random walk with restart (RWR) (Page et al., 1999) and its extension, biased random walk with restart (BRWR), have been employed in various domains such as node representation learning (Perozzi et al., 2014) and graph traversals (Ahrabian et al., 2020). In BRWR, a random walker performs random walks in a graph from the source node. For each iteration, the walker moves from the current node u to either (i) source with a probability of p_r , or (ii) one of the neighbors of u with a probability of $1 - p_r$, where p_r is a hyperparameter. In case (ii), the probability of selecting one of the neighbors is decided by a domain-specific probability distribution, whereas one is selected uniformly at random in RWR. To our knowledge, we are the first to extract a subgraph of KG via BRWR to utilize the subgraph as a mini-batch during training.

3 Motivation

To demonstrate the limitations of text-based methods exhibiting competitive performance such as SimKGC (Wang et al., 2022a) and StAR (Wang et al., 2021a), we investigate the characteristics of false positive (FP) triples which are ranked by these models higher than corresponding true triples, on two widely-used datasets WN18RR and FB15k-237. Our analysis draws two conclusions.

First, the closer the tail and head of a false triple are to each other in the KG, the more likely the false triple is to be ranked higher than the corresponding true triple. Figure 1 illustrates the distribution of distance, i.e., the length of the shortest path, between the head and tail of a FP triple, where y -axis represents the FP ratio¹ for each distance. For StAR and SimKGC, the FP ratio dramatically grows as the distance decreases (see green and red bars in Figure 1). These findings highlight the importance

¹(the number of FPs with a specific head-to-tail distance) / (the number of pairs of entities in the KG with the same distance).

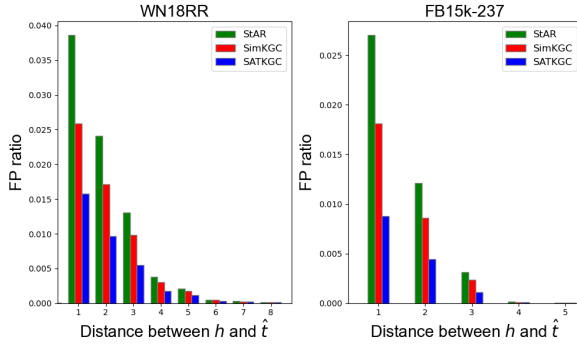


Figure 1: False positive (FP) ratio against the distance (i.e., length of the shortest path) between head and tail of a FP triple in KG across different text-based methods.

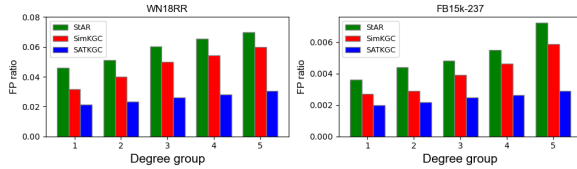


Figure 2: False positive (FP) ratio against the degree of head for a FP triple across different text-based methods.

of considering the proximity of two entities of a negative triple in KGs for text-based methods to distinguish a positive triple from the negative.

Second, we discover that the higher the degree of the head in a false triple is, the more likely the false triple is to be ranked higher than the corresponding true triple. Figure 2 illustrates the distribution of the degree of heads of FP triples. The FPs are sorted in ascending order of the degrees, and then they are divided into five groups such that each group contains an equal number of distinct degrees. The y -axis represents the FP ratio² in each degree group. The FP ratio for StAR and SimKGC increases as the degree of the head grows (see green and red bars in Figure 2). This indicates that the existing text-based methods have difficulty in predicting correct tails for missing triples with the high-degree heads. Hence, the degree can be taken into account to enhance the performance of text-based methods.

Our proposed framework (dubbed SATKGC) tackles the above two phenomena³, thereby significantly reducing the FPs for all distances and all degree groups compared to the existing methods (see blue bars in Figures 1 and 2).

²(the average number of FPs whose head’s degree falls into each group) / (the number of entities in the KG whose degree falls into each group)

³The trends in Figures 1 and 2 are also confirmed on Wikidata5M and NELL-995.

4 Method

We propose a novel training framework for KGC that captures the structural inductive bias of the KG, based on the aforementioned observations.

Figure 3 illustrates the overview of our framework. First, for every triple, a subgraph is extracted around that triple from the KG, performed before training (Section 4.1). During training, we keep track of the number of visits for every triple. For each iteration, a subgraph is selected based on that number, and then all forward and inverse triples in the subgraph are fetched as a mini-batch B to a model (Section 4.2). We adopt the bi-encoder architecture (Wang et al., 2022b) as a backbone, which uses pre-trained BERT (Devlin et al., 2018) as encoders. Specifically, $Encoder_{hr}$ and $Encoder_t$ take the text, i.e., name and description, of (h, r) and t as input, and produce their embeddings x_{hr} and x_t respectively. We then calculate the cosine similarity between x_{hr} and x_t for every (h, r) and t in the mini-batch, and perform contrastive learning based on two structure-aware factors (Section 4.3). The model inference is described in Appendix A.

4.1 Random-Walk Based Subgraph Sampling

First, we aim to extract subgraphs from the KG to treat all the triples in the extracted subgraph as a mini-batch for training. For each triple in the KG, we perform BRWR starting from that triple called a center triple, and the triples visited by BRWR composes an extracted subgraph as follows: (i) for each center triple, either head h or tail t of the center triple is selected as the start entity s based on an inverse degree distribution of h and t , i.e., $\frac{|N(x)|^{-1}}{|N(h)|^{-1}+|N(t)|^{-1}}$, where $x \in \{h, t\}$ and $N(x)$ denotes a set of x ’s neighbors; (ii) next, we perform BRWR from s until we sample M triples where M is a predefined maximum number (e.g., 10,000). For each iteration in BRWR, a random walker moves from the current node to either s with a probability of p_r or one of the neighbors of the current node with a probability of $1 - p_r$. We define the probability of selecting one of u ’s neighbors $v \in N(u)$ as $p_v = \frac{|N(v)|^{-1}}{\sum_{v \in N(u)} |N(v)|^{-1}}$, which is a normalized inverse degree distribution of the neighbors. Figures 4a and 4b show the running example of step (i) and an iteration of step (ii).

Performed before the model training, this subgraph sampling algorithm can extract many distinct entities due to the inverse degree distribution,

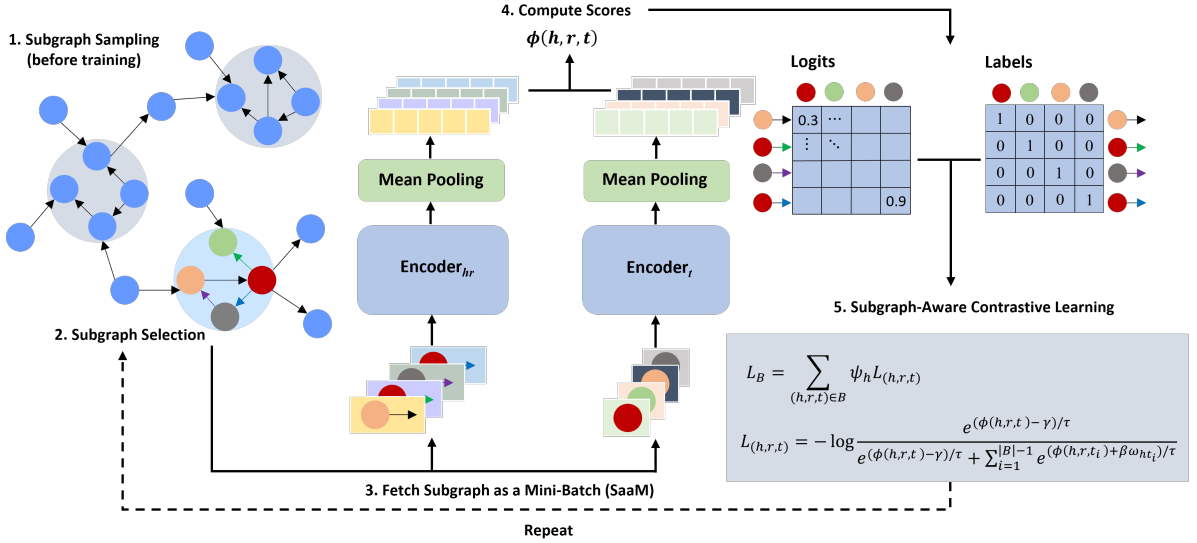


Figure 3: Overview of the proposed training framework, which consists of: (i) sampling subgraphs from KG (before training); (ii) selecting a subgraph; (iii) fetching a mini-batch of triples in the subgraph; (iv) calculating a similarity between embeddings of every (head, relation) pair and every tail in the mini-batch; (v) contrastive learning via InfoNCE loss incorporated with two structure-aware factors.

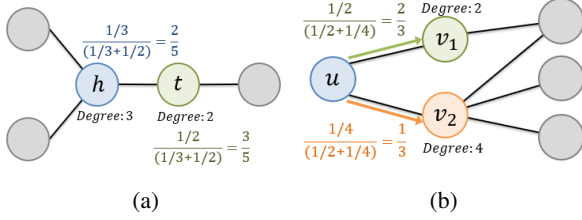


Figure 4: Example of BRWR-based subgraph sampling; (a) probability of selecting the start entity s between h and t of a center triple, where t with a lower degree is more likely to be selected as s than h ; (b) probability of selecting a neighbor of current entity u . A random walker is more likely to move to v_1 than to v_2 whose degree is larger than v_1 .

which will be validated in Section 5.5.

4.2 Subgraph as a Mini-Batch

In this subsection, we describe our training framework dubbed **Subgraph as a Mini-batch (SaaM)**. We count the number of visits for all triples in the training set T throughout the training process. For every iteration, we select the subgraph whose center triple is the least frequently visited, to prioritize unpopular and peripheral triples. The rationale behind this selection will be elaborated in Section 6.2. Next, we randomly select $|B|/2$ triples from the subgraph, and feed to the model a mini-batch B of the these selected triples (h, r, t) and their inverse triples (t, r^{-1}, h) . For every positive triple $(h, r, t) \in B$, we obtain negative triples (h, r, \hat{t}) with t replaced by $|B| - 1$ tails \hat{t} of the other triples

in B . As per our observation in Figure 1, these negative triples are likely to be hard negatives, which will facilitate contrastive learning.

To introduce a concept corresponding to an epoch in our training framework, let iterating above process for $|T|/|B|$ times, i.e., selecting and feeding $|T|/|B|$ subgraphs, be a “phase” as opposed to an epoch that visits every triple exactly once.

4.3 Subgraph-Aware Contrastive Learning

For effective contrastive learning, we propose to incorporate two structure-aware factors into InfoNCE loss with additive margin (Chen et al., 2020; Yang et al., 2019) over a mini-batch: (a) structural hardness of negatives for each positive triple, and (b) structural hardness of head entities in the mini-batch. These two factors are simply obtained from the topological structure of the subgraph, while incurring a minimal computational overhead overall.

4.3.1 Structural Hardness of Negative Triples

Entities close to each other are more likely to be related than entities far away from each other. Although text-based KGC methods capture semantic relations within the text of triples, they overlook capturing the proximity between two entities in a negative triple in KGs. To tackle this problem, we propose a novel InfoNCE loss that penalizes structurally hard negative triples. For each positive triple (h, r, t) in a mini-batch B of SaaM, the loss function $L_{(h,r,t)}$ is defined as

$$L_{(h,r,t)} = -\log \frac{e^{(\phi(h,r,t) - \gamma)/\tau}}{e^{(\phi(h,r,t) - \gamma)/\tau} + \sum_{i=1}^{|B|-1} e^{(\phi(h,r,t_i) + \beta \omega_{ht_i})/\tau}} \quad (1)$$

where γ is an additive margin, a temperature parameter τ adjusts the importance of negatives, structural hardness ω_{ht_i} stands for how hard a negative triple (h, r, t_i) is in terms of the structural relation between h and t_i in the KG, and β is a trainable parameter that adjusts the relative importance of ω_{ht_i} . Specifically, we define ω_{ht_i} as the reciprocal of the distance (i.e., length of the shortest path) between h and t_i to impose a larger weight ω_{ht_i} to the negative triple with a shorter distance between h and t_i , which serves as a harder negative triple.

Since computing the exact distance between every head and every tail in B may spend considerable time, in our implementation, we calculate the approximate distance between h and t_i , i.e., the multiplication of two distances: (d1) the distance between h and head h_c of the center triple of B , and (d2) the distance between t_i and h_c . For this, the distance between h_c and every entity in B is pre-computed before training, the multiplication between the two distances is performed in parallel during training, which requires a minimal computational overhead.⁴

4.3.2 Structural Hardness of Entities

For many triples with the same head in the KG, varying only relation r in $(h, r, ?)$ may lead to different correct tails with various semantic contexts. The text-based KGC methods may find it difficult to predict the correct tail for these triples, as their head-relation encoders may generate less diverse embeddings for (h, r) due to much shorter text of relation r than entity h .

To encourage the text-based method to more sensitively adapt to varying relations for many triples with the identical head, we propose a novel loss weighting strategy that penalizes structurally hard head entities. For each triple in a mini-batch B in SaaM, mini-batch loss L_B is defined as

$$L_B = \sum_{(h,r,t) \in B} \psi_h L_{(h,r,t)} \quad (2)$$

where structural hardness ψ_h of head h indicates how difficult (h, r, t) is in terms of the structural

⁴We conducted experiments using the exact distance and different approximate distances, e.g., the sum of (d1) and (d2), but the performance gap between all the methods is very marginal.

dataset	#entity	#relation	#train	#valid	#test
WN18RR	40,943	11	86,835	3,034	3,134
NELL-995	74,332	200	149,678	543	3,992
FB15k-237	14,541	237	272,115	17,535	20,466
Wikidata5M-Trans	4,594,485	822	20,614,279	5,163	5,163
Wikidata5M-Ind	4,579,609	822	20,496,514	6,699	6,894

Table 1: Statistics of datasets.

property of h in the KG. Specifically, we define ψ_h as $\log(d_h + 1)$ where d_h represents the degree of h , and adding one to d_h can prevent ψ_h from becoming zero when $d_h = 1$. To sum up, ψ_h ensures that the triples whose heads have a larger degree contribute more significantly to L_B .

5 Experiments

5.1 Experimental Setup

For evaluation we adopt widely-used KG datasets WN18RR, FB15k-237, NELL-995 and Wikidata5M. Table 1 shows their statistics, and more details are provided in Appendix C.

For every incomplete triple in the test set, we compute mean reciprocal rank (MRR) and Hits@ k where $k \in \{1, 3, 10\}$ as evaluation metrics based on the rank of the correct entity among all the entities in the KG. We use the mean of the forward and backward prediction results as the final performance measure. Implementation details are described in Appendix D.

5.2 Main Results

We compare SATKGC with existing embedding-based and text-based approaches. Table 2 shows the results on WN18RR, NELL-995, and FB15k-237, and Table 3 shows the results on Wikidata5M-Trans and Wikidata5M-Ind.⁵ SATKGC denotes the bi-encoder architectures trained by our learning framework in Figure 3. Note that Table 2 presents the performance of the latest baselines, and the complete results for all baselines compared with ours are found in Appendix K. SATKGC consistently outperforms all the existing methods on all the datasets except MRR on NELL-995. SATKGC demonstrates significantly higher MRR and Hits@1 than other baselines especially on WN18RR and FB15k-237. The small performance improvement of our method on NELL-995 stems from the limited textual context in this dataset, unlike other datasets. Nevertheless, SATKGC is the runner-up lagged only 0.001 behind CompoundE

⁵The results of GHN on NELL-995 are unavailable due to a lack of access to the requisite codes.

Approach	WN18RR				NELL-995				FB15k-237			
	MRR	Hits@1	Hits@3	Hits@10	MRR	Hits@1	Hits@3	Hits@10	MRR	Hits@1	Hits@3	Hits@10
<i>Embedding-based approach</i>												
TuckER (Balazevic et al., 2019)	0.466	0.432	0.478	0.518	0.423	0.363	0.455	0.536	<u>0.361</u>	0.265	0.391	0.538
RotatE (Sun et al., 2019)	0.471	0.421	0.490	0.568	0.411	0.350	0.439	0.522	0.335	0.243	0.374	0.529
KG Tuner (Zhang et al., 2022)	0.481	0.438	0.499	0.556	0.428	0.371	0.458	0.544	0.345	0.252	0.381	0.534
CompoundE (Ge et al., 2023)	0.492	0.452	0.510	0.570	0.434	<u>0.381</u>	0.466	0.550	0.350	0.262	0.390	<u>0.547</u>
CSProm-KG (Chen et al., 2023)	0.569	0.520	0.590	0.675	0.422	<u>0.381</u>	<u>0.474</u>	0.535	0.355	0.261	0.389	0.531
<i>Text-based approach</i>												
StAR (Wang et al., 2021a)	0.398	0.238	0.487	0.698	0.419	0.238	0.395	0.433	0.288	0.195	0.313	0.480
HaSa (Zhang et al., 2023a)	0.538	0.444	0.588	0.713	0.411	0.310	0.431	0.524	0.304	0.220	0.325	0.483
KG-S2S (Chen et al., 2022)	0.572	0.529	0.595	0.663	0.416	0.311	0.421	0.519	0.337	0.255	0.374	0.496
SimKGC (Wang et al., 2022a)	0.671	0.580	<u>0.729</u>	0.811	0.425	0.353	0.447	0.531	0.340	0.252	0.365	0.515
GHN (Qiao et al., 2023) [†]	0.678	0.596	0.719	<u>0.821</u>	-	-	-	-	0.339	0.251	0.364	0.518
<i>Ensemble approach</i>												
StAR (Wang et al., 2021a)	0.520	0.456	0.509	0.707	0.415	0.311	0.402	0.510	0.332	0.229	0.387	0.526
SATKGC-SPW-DW	0.672	0.605	0.714	0.811	0.411	0.310	0.431	0.524	0.345	0.225	0.367	0.520
SATKGC-DW	0.679	0.609	0.723	0.813	0.429	0.361	0.466	0.551	0.351	0.261	0.372	0.525
SATKGC-SPW	0.681	0.612	<u>0.729</u>	0.820	0.431	0.369	0.472	<u>0.556</u>	0.359	0.271	<u>0.393</u>	0.538
SATKGC	<u>0.689</u>	<u>0.621</u>	<u>0.731</u>	<u>0.823</u>	<u>0.433</u>	<u>0.389</u>	<u>0.476</u>	<u>0.560</u>	<u>0.368</u>	<u>0.276</u>	<u>0.401</u>	<u>0.548</u>

Table 2: KGC results for the WN18RR, NELL-995, and FB15k-237 datasets. “SPW” and “DW” refer to shortest path weight and degree weight respectively. The best and second-best performances are denoted in **bold** and underlined respectively. [†]: numbers are from Qiao et al. (2023).

Approach	Wikidata5M-Trans				Wikidata5M-Ind			
	MRR	Hits@1	Hits@3	Hits@10	MRR	Hits@1	Hits@3	Hits@10
<i>Embedding-based approach</i>								
TransE (Bordes et al., 2013)	0.253	0.170	0.311	0.392	-	-	-	-
RotatE (Sun et al., 2019)	0.290	0.234	0.322	0.390	-	-	-	-
<i>Text-based approach</i>								
DKRL (Xie et al., 2016)	0.160	0.120	0.181	0.229	0.231	0.059	0.320	0.546
KEPLER (Wang et al., 2021c)	0.212	0.175	0.221	0.276	0.403	0.225	0.517	0.725
BLP-ComplEx (Daza et al., 2021)	-	-	-	-	0.491	0.261	0.670	0.881
BLP-SimplE (Daza et al., 2021)	-	-	-	-	0.490	0.283	0.641	0.868
SimKGC (Wang et al., 2022a)	0.358	<u>0.313</u>	<u>0.376</u>	<u>0.441</u>	0.714	0.609	<u>0.785</u>	<u>0.917</u>
SATKGC	0.404	0.361	0.423	0.479	0.763	0.659	0.809	0.927

Table 3: KGC results for Wikidata5M-Trans (transductive setting) and Wikidata5M-Ind (inductive setting). The results for embedding-based approach on Wikidata5M-ind are missing as they cannot be used in the inductive setting. Additionally, BLP-ComplEx (Daza et al., 2021) and BLP-SimplE (Daza et al., 2021) results on Wikidata5M-Trans are missing because they are inherently targeted for inductive KGC.

FB15K-237N				
Models	MRR	Hits@1	Hits@3	Hits@10
KoPA (Zhang et al., 2023c)	0.483	0.344	0.559	0.721
SATKGC	0.668	0.557	0.742	0.858

Table 4: KGC results on FB15K-237N. A correct tail is ranked among 1,000 randomly-selected entities due to the long inference time of KoPA.

for MRR on NELL-995, while outperforming all baselines on the remaining metrics.

As shown in Table 3, SATKGC demonstrates its applicability to large-scale KGs, and achieves strong performance in both inductive and transductive settings.⁶ SATKGC significantly outper-

forms the baselines on Wikidata5M-Ind, reaching MRR of 0.763 and Hits@1 of 0.659.⁷ In the transductive setting, performance degrades in the order of WN18RR, Wikidata5M-Trans, and FB15k-237, showing that a higher average degree of entities tends to negatively affect performance.

To compare our framework employing BERTs with a LLM-based model, we evaluate the KGC performance of KoPA (Zhang et al., 2023c), which adopts Alpaca (Taori et al., 2023) fine-tuned with LoRA (Hu et al., 2021) as its backbone, on the FB15k-237N dataset (Zhang et al., 2023c). Since KoPA cannot perform inference for all queries within a reasonable time, i.e., 111 hours expected,

⁶Baselines listed in Table 2 but not in Table 3 could not be evaluated on Wikidata5M due to out-of-memory for StAR and CSProm-KG, or unreasonably large training time, i.e., more than 100 hours expected, for the remaining baselines.

⁷Wikidata5M-Ind shows better performance than Wikidata5M-Trans, because a model ranks 7,475 entities in the test set for Wikidata5M-Ind while ranking about 4.6 million entities for Wikidata5M-Trans.

WN18RR					
Encoders	MRR	Hits@1	Hits@3	Hits@10	Parameters
BERT-base	0.689	0.621	0.731	0.823	220M
DeBERTa-base	0.689	0.631	0.736	0.832	280M
BERT-large	0.685	0.619	0.723	0.817	680M
DeBERTa-large	0.706	0.638	0.759	0.854	800M

NELL-995					
Encoders	MRR	Hits@1	Hits@3	Hits@10	Parameters
BERT-base	0.433	0.389	0.476	0.560	220M
DeBERTa-base	0.434	0.388	0.478	0.559	280M
BERT-large	0.432	0.367	0.475	0.541	680M
DeBERTa-large	0.426	0.368	0.428	0.551	800M

Table 5: Performance comparison for different encoders.

we rank the correct tail among 1,000 randomly selected entities for both KoPA and SATKGC. As shown in Table 4, SATKGC outperforms KoPA on all metrics, demonstrating that LLMs do not necessarily produce superior results on KGC.

5.3 Ablation study

To show the contributions of applying SaaM and adding the two weighting factors to InfoNCE loss, we compare results of four different settings including SATKGC in Table 2: SATKGC-SPW-DW denotes applying only SaaM and using original InfoNCE loss, SATKGC-SPW represents applying SaaM and the degree factor ψ_h , and SATKGC-DW represents applying SaaM and the distance factor ω_{ht_i} . SATKGC-SPW-DW already shows higher Hits@1 than other baselines on WN18RR, which highlights that SaaM alone can lead to performance improvement. The efficacy of SaaM is further evidenced in Appendix F. Between SATKGC-SPW and SATKGC-DW, SATKGC-SPW achieves higher performance, which indicates that the degree factor contributes more than the distance factor.

5.4 Performance Across Encoders

To investigate the impact of the encoder architecture and the number of model parameters, we conduct experiments replacing BERT-base in SATKGC with BERT-large, DeBERTa-base, and DeBERTa-large (He et al., 2020). Table 5 presents the results. SATKGC is highly compatible with different encoders, showing the competitive performance. DeBERTa-large fine-tuned by SATKGC achieves the best performance on WN18RR. In addition, an increase in the number of model parameters may not necessarily result in enhanced performance on KGC, e.g., BERT-large on WN18RR, and BERT-large and DeBERTa-large on NELL-995 underperform the smaller encoders.

WN18RR				
Methods	MRR	Hits@1	Hits@3	Hits@10
RWR	0.682	0.620	0.728	0.821
BRWR	0.689	0.621	0.731	0.823
BRWR_P	0.673	0.610	0.726	0.810
MCMC	0.676	0.609	0.716	0.802

FB15k-237				
Methods	MRR	Hits@1	Hits@3	Hits@10
RWR	0.355	0.264	0.382	0.532
BRWR	0.368	0.279	0.403	0.548
BRWR_P	0.347	0.258	0.376	0.526
MCMC	0.346	0.259	0.376	0.521

Table 6: Experiments comparing subgraph sampling methods on WN18RR and FB15k-237.

5.5 Comparing Sampling Methods

We investigate how model performance varies depending on the probability distribution p_v used for neighbor selection in Section 4.1.⁸ We compare the performance of SATKGC using p_v in subgraph sampling with two variants, one with p_v replaced by the uniform distribution (dubbed RWR) and the other with p_v replaced by the degree proportional distribution (dubbed BRWR_P). Table 6 shows the results. The three methods mostly outperform existing KGC models in Hits@1, with BRWR performing best. BRWR_P performs the worst, likely due to many duplicate entities in the extracted subgraphs sampled from the degree-proportional distribution. We also employ a Markov chain Monte Carlo (MCMC) based subgraph sampling method (Yang et al., 2020), referred to as MCMC (see details of MCMC in Appendix B). Note that in Table 2, MCMC outperforms other methods in terms of Hits@1 on WN18RR.

6 Analysis

6.1 Analysis on Negative Triples

Figure 5 shows how the cosine similarity distribution of in-batch negative triples varies depending on the epoch of SimKGC, and the phase of SATKGC for FB15k-237. SATKGC encounters consistently more hard negatives with scores from 0.2 to 1.0 than SimKGC, though the majority of the scores range from -0.2 to 0.2 by the end of training for both methods.⁹ We speculate that SATKGC ends up with distinguishing positives from the hard

⁸Recall that in our BRWR algorithm, a random walker selects one of the neighbors v of a current node based on the inverse degree distribution p_v .

⁹This trend is also observed in WN18RR.

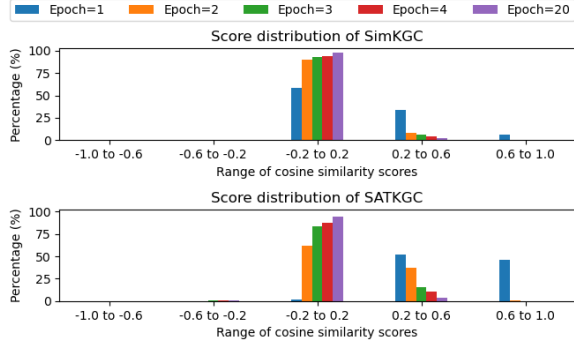


Figure 5: Percentage of in-batch negative triples on FB15k-237 according to the range of cosine similarity scores predicted by SimKGC for different epochs and by SATKGC for different phases.

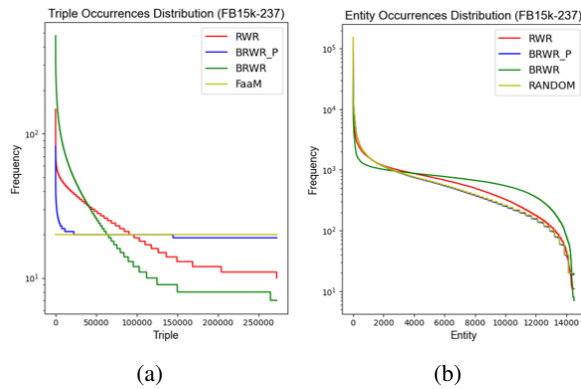


Figure 6: (a) Number of occurrences of triples; (b) number of occurrences of entities. Both are counted throughout the entire training process for RANDOM and the SaaM variants, i.e., RWR, BRWR_P, and BRWR.

negatives sampled from the subgraphs of a KG, as opposed to SimKGC which employs randomly-sampled easy negatives. The effectiveness using only negatives from SaaM in enhancing performance is demonstrated in Appendix G.

Based on our analysis, only 2.83% and 4.42% of the true triples ranked within the top 10 by SimKGC drop out of the top 10 for SATKGC on WN18RR and FB15k-237, respectively. In contrast, 34.87% and 13.03% of the true triples dropping out of the top 10 for SimKGC are ranked within the top 10 by SATKGC. This indicates that SATKGC effectively samples hard negatives while reducing false negatives.

6.2 Skewness of Occurrences

Figures 6a and 6b show the number of visits of every triple and every entity, respectively, in the training process for RANDOM and the SaaM variants: RWR, BRWR_P, and BRWR. RANDOM, adopted in all the baselines, denotes selecting a mini-batch of triples at random without replace-

ment. Triples and entities are sorted by descending frequency. Figure 6a demonstrates that RANDOM exhibits a uniform distribution, while RWR, BRWR_P, and BRWR display varying degrees of skewness, with BRWR being the most skewed and BRWR_P the least. Figure 6b illustrates that BRWR is the least skewed whereas RANDOM shows the most skewed distribution. As a result, a larger skewness in the distribution of number of visits for triples in turn leads to more equally visiting entities, thus improving the performance.¹⁰

Further analysis reinforces this finding. In FB15k-237, the average degree of FP triples’ tails is 75 for SATKGC and 63 for SimKGC. A smaller portion of low-degree tails for SATKGC than for SimKGC indicates that exposure to more low-degree entities \hat{t} in training helps the model position their embeddings farther from the (h, r) embeddings for negative triples (h, r, \hat{t}) , as SATKGC visits low-degree entities more often during training than RANDOM for SimKGC.¹¹

For BRWR in Figure 6a, we examine the structural characteristics on sets S_m and S_l of entities in 1,000 most and least frequent triples, respectively. The entities in S_m have an average degree of 11.1, compared to 297.3 for those in S_l . The betweenness centrality¹² averages around 5.2×10^{-5} for S_m and 8.2×10^{-4} for S_l . These observations implies that SaaM prioritizes visiting unpopular and peripheral triples in the KG over focusing on information-rich triples.

7 Conclusion

In this paper, we propose a generic training scheme and a new contrastive learning method for KGC. Harmonizing (i) SaaM using a subgraph of KG as a mini-batch, and (ii) contrastive learning that incorporates the structural hardness of the KG into fine-tuning PLMs helps learning the contextual text embeddings aware of the difficulty in the structural context of the KG. Our findings imply that unequally feeding triples in training and leveraging the unique characteristics of KG lead to the effective text-based KGC method, achieving state-of-the-art performance on the four KG benchmarks.

¹⁰The similar trends are shown on WN18RR.

¹¹This is also confirmed in all the other datasets.

¹²The betweenness centrality of node v is the number of shortest paths that pass through v in the graph divided by the total number of shortest paths between all pairs of nodes, which measures v ’s importance in the graph.

Limitations

While our training scheme efficiently samples many hard negatives from subgraphs, BRWR incurs a computational overhead to extract subgraphs from Wikidata5M before training (see Appendix E). However, note that this algorithm can be efficiently parallelized or replaced by a simpler one.

References

Kian Ahrabian, Aarash Feizi, Yasmin Salehi, William L. Hamilton, and Avishek Joey Bose. 2020. [Structure aware negative sampling in knowledge graphs](#). In *Proceedings of the 2020 Conference on Empirical Methods in Natural Language Processing (EMNLP)*, pages 6093–6101, Online. Association for Computational Linguistics.

Ivana Balazevic, Carl Allen, and Timothy Hospedales. 2019. [Tucker: Tensor factorization for knowledge graph completion](#). In *Proceedings of the 2019 Conference on Empirical Methods in Natural Language Processing and the 9th International Joint Conference on Natural Language Processing (EMNLP-IJCNLP)*. Association for Computational Linguistics.

Antoine Bordes, Nicolas Usunier, Alberto Garcia-Duran, Jason Weston, and Oksana Yakhnenko. 2013. Translating embeddings for modeling multi-relational data. *Advances in neural information processing systems*, 26.

Chen Chen, Yufei Wang, Bing Li, and Kwok-Yan Lam. 2022. [Knowledge is flat: A Seq2Seq generative framework for various knowledge graph completion](#). In *Proceedings of the 29th International Conference on Computational Linguistics*, pages 4005–4017, Gyeongju, Republic of Korea. International Committee on Computational Linguistics.

Chen Chen, Yufei Wang, Aixin Sun, Bing Li, and Kwok-Yan Lam. 2023. [Dipping PLMs sauce: Bridging structure and text for effective knowledge graph completion via conditional soft prompting](#). In *Findings of the Association for Computational Linguistics: ACL 2023*, pages 11489–11503, Toronto, Canada. Association for Computational Linguistics.

Ting Chen, Simon Kornblith, Mohammad Norouzi, and Geoffrey Hinton. 2020. [A simple framework for contrastive learning of visual representations](#).

Daniel Daza, Michael Cochez, and Paul Groth. 2021. [Inductive entity representations from text via link prediction](#). In *Proceedings of the Web Conference 2021*, WWW ’21, page 798–808, New York, NY, USA. Association for Computing Machinery.

Jacob Devlin, Ming-Wei Chang, Kenton Lee, and Kristina Toutanova. 2018. Bert: Pre-training of deep bidirectional transformers for language understanding. *arXiv preprint arXiv:1810.04805*.

Hongchao Fang, Sicheng Wang, Meng Zhou, Jiayuan Ding, and Pengtao Xie. 2020. [Cert: Contrastive self-supervised learning for language understanding](#).

Tianyu Gao, Xingcheng Yao, and Danqi Chen. 2021. [SimCSE: Simple contrastive learning of sentence embeddings](#). In *Proceedings of the 2021 Conference on Empirical Methods in Natural Language Processing*, pages 6894–6910, Online and Punta Cana, Dominican Republic. Association for Computational Linguistics.

Xiou Ge, Yun Cheng Wang, Bin Wang, and C.-C. Jay Kuo. 2023. [Compounding geometric operations for knowledge graph completion](#). In *Proceedings of the 61st Annual Meeting of the Association for Computational Linguistics (Volume 1: Long Papers)*, pages 6947–6965, Toronto, Canada. Association for Computational Linguistics.

Ayaan Haque, Hankyu Moon, Heng Hao, Sima Didiari, Jae Oh Woo, and Patrick Bangert. 2022. [Self-supervised contrastive representation learning for 3d mesh segmentation](#).

He He, Anusha Balakrishnan, Mihail Eric, and Percy Liang. 2017. Learning symmetric collaborative dialogue agents with dynamic knowledge graph embeddings. *arXiv preprint arXiv:1704.07130*.

Pengcheng He, Xiaodong Liu, Jianfeng Gao, and Weizhu Chen. 2020. Deberta: Decoding-enhanced bert with disentangled attention. *arXiv preprint arXiv:2006.03654*.

Edward J Hu, Yelong Shen, Phillip Wallis, Zeyuan Allen-Zhu, Yuanzhi Li, Shean Wang, Lu Wang, and Weizhu Chen. 2021. Lora: Low-rank adaptation of large language models. *arXiv preprint arXiv:2106.09685*.

Shaoxiong Ji, Shirui Pan, Erik Cambria, Pekka Marttinen, and S Yu Philip. 2021. A survey on knowledge graphs: Representation, acquisition, and applications. *IEEE transactions on neural networks and learning systems*, 33(2):494–514.

Yannis Kalantidis, Mert Bulent Sariyildiz, Noe Pion, Philippe Weinzaepfel, and Diane Larlus. 2020. Hard negative mixing for contrastive learning. *Advances in Neural Information Processing Systems*, 33:21798–21809.

Bosung Kim, Taesuk Hong, Youngjoong Ko, and Jungyun Seo. 2020. [Multi-task learning for knowledge graph completion with pre-trained language models](#). In *Proceedings of the 28th International Conference on Computational Linguistics*, pages 1737–1743, Barcelona, Spain (Online). International Committee on Computational Linguistics.

Danyang Liu, Jianxun Lian, Zheng Liu, Xiting Wang, Guangzhong Sun, and Xing Xie. 2021. Reinforced anchor knowledge graph generation for news recommendation reasoning. In *Proceedings of the 27th ACM SIGKDD Conference on Knowledge Discovery & Data Mining*, pages 1055–1065.

George A. Miller. 1992. WordNet: A lexical database for English. In *Speech and Natural Language: Proceedings of a Workshop Held at Harriman, New York, February 23-26, 1992*.

Maximilian Nickel, Volker Tresp, and Hans-Peter Kriegel. 2011. A three-way model for collective learning on multi-relational data. In *Proceedings of the 28th International Conference on Machine Learning (ICML-11)*, pages 809–816.

Lawrence Page, Sergey Brin, Rajeev Motwani, and Terry Winograd. 1999. The pagerank citation ranking : Bringing order to the web. In *The Web Conference*.

Bryan Perozzi, Rami Al-Rfou, and Steven Skiena. 2014. Deepwalk: Online learning of social representations. In *Proceedings of the 20th ACM SIGKDD international conference on Knowledge discovery and data mining*, pages 701–710.

Zile Qiao, Wei Ye, Dingyao Yu, Tong Mo, Weiping Li, and Shikun Zhang. 2023. Improving knowledge graph completion with generative hard negative mining. In *Findings of the Association for Computational Linguistics: ACL 2023*, pages 5866–5878, Toronto, Canada. Association for Computational Linguistics.

Joshua David Robinson, Ching-Yao Chuang, Suvrit Sra, and Stefanie Jegelka. 2021. Contrastive learning with hard negative samples. In *International Conference on Learning Representations*.

Zhiqing Sun, Zhi-Hong Deng, Jian-Yun Nie, and Jian Tang. 2019. Rotate: Knowledge graph embedding by relational rotation in complex space. In *International Conference on Learning Representations*.

Rohan Taori, Ishaan Gulrajani, Tianyi Zhang, Yann Dubois, Xuechen Li, Carlos Guestrin, Percy Liang, and Tatsunori B. Hashimoto. 2023. Stanford alpaca: An instruction-following llama model. https://github.com/tatsu-lab/stanford_alpaca.

Théo Trouillon, Johannes Welbl, Sebastian Riedel, Éric Gaussier, and Guillaume Bouchard. 2016. Complex embeddings for simple link prediction. In *International conference on machine learning*, pages 2071–2080. PMLR.

Ashish Vaswani, Noam Shazeer, Niki Parmar, Jakob Uszkoreit, Llion Jones, Aidan N Gomez, Łukasz Kaiser, and Illia Polosukhin. 2017. Attention is all you need. *Advances in neural information processing systems*, 30.

Bo Wang, Tao Shen, Guodong Long, Tianyi Zhou, Ying Wang, and Yi Chang. 2021a. Structure-augmented text representation learning for efficient knowledge graph completion. In *Proceedings of the Web Conference 2021*, WWW '21. ACM.

Liang Wang, Wei Zhao, Zhuoyu Wei, and Jingming Liu. 2022a. Simkgc: Simple contrastive knowledge graph completion with pre-trained language models.

Liang Wang, Wei Zhao, Zhuoyu Wei, and Jingming Liu. 2022b. SimKGC: Simple contrastive knowledge graph completion with pre-trained language models. In *Proceedings of the 60th Annual Meeting of the Association for Computational Linguistics (Volume 1: Long Papers)*, pages 4281–4294, Dublin, Ireland. Association for Computational Linguistics.

Xiaozhi Wang, Tianyu Gao, Zhaocheng Zhu, Zhengyan Zhang, Zhiyuan Liu, Juanzi Li, and Jian Tang. 2021b. KEPLER: A unified model for knowledge embedding and pre-trained language representation. *Transactions of the Association for Computational Linguistics*, 9:176–194.

Xiaozhi Wang, Tianyu Gao, Zhaocheng Zhu, Zhengyan Zhang, Zhiyuan Liu, Juanzi Li, and Jian Tang. 2021c. Kepler: A unified model for knowledge embedding and pre-trained language representation. *Transactions of the Association for Computational Linguistics*, 9:176–194.

Yiran Wang, Hiroyuki Shindo, Yuji Matsumoto, and Taro Watanabe. 2021d. Structured refinement for sequential labeling. In *Findings of the Association for Computational Linguistics: ACL-IJCNLP 2021*, pages 1873–1884, Online. Association for Computational Linguistics.

Zhirong Wu, Yuanjun Xiong, Stella Yu, and Dahua Lin. 2018. Unsupervised feature learning via non-parametric instance-level discrimination.

Ruobing Xie, Zhiyuan Liu, Jia Jia, Huanbo Luan, and Maosong Sun. 2016. Representation learning of knowledge graphs with entity descriptions. *Proceedings of the AAAI Conference on Artificial Intelligence*, 30(1).

Chenyan Xiong, Russell Power, and Jamie Callan. 2017. Explicit semantic ranking for academic search via knowledge graph embedding. In *Proceedings of the 26th international conference on world wide web*, pages 1271–1279.

Bishan Yang, Scott Wen-tau Yih, Xiaodong He, Jian-feng Gao, and Li Deng. 2015. Embedding entities and relations for learning and inference in knowledge bases. In *Proceedings of the International Conference on Learning Representations (ICLR) 2015*.

Yinfei Yang, Gustavo Hernandez Abrego, Steve Yuan, Mandy Guo, Qinlan Shen, Daniel Cer, Yun-Hsuan Sung, Brian Strope, and Ray Kurzweil. 2019. Improving multilingual sentence embedding using bi-directional dual encoder with additive margin softmax. *arXiv preprint arXiv:1902.08564*.

Zhen Yang, Ming Ding, Chang Zhou, Hongxia Yang, Jingren Zhou, and Jie Tang. 2020. Understanding negative sampling in graph representation learning.

Liang Yao, Chengsheng Mao, and Yuan Luo. 2019. Kgbert: Bert for knowledge graph completion. *arXiv preprint arXiv:1909.03193*.

Fuzheng Zhang, Nicholas Jing Yuan, Defu Lian, Xing Xie, and Wei-Ying Ma. 2016. Collaborative knowledge base embedding for recommender systems. In *Proceedings of the 22nd ACM SIGKDD international conference on knowledge discovery and data mining*, pages 353–362.

Honggen Zhang, June Zhang, and Igor Molybog. 2023a. **Hasa: Hardness and structure-aware contrastive knowledge graph embedding**.

Junlei Zhang, Zhenzhong Lan, and Junxian He. 2023b. **Contrastive learning of sentence embeddings from scratch**.

Yichi Zhang, Zhuo Chen, Wen Zhang, and Huajun Chen. 2023c. Making large language models perform better in knowledge graph completion. *arXiv preprint arXiv:2310.06671*.

Yongqi Zhang, Zhanke Zhou, Quanming Yao, and Yong Li. 2022. **Kgtuner: Efficient hyper-parameter search for knowledge graph learning**.

A Inference

For inference, the bi-encoder model calculates the cosine similarity between \mathbf{x}_{hr} for a given $(h, r, ?)$ and \mathbf{x}_t for all entities t . Then the tails with the top-k largest cosine similarities are answers. For a single pair, we need $|E|$ forward passes of $Encoder_t$ to obtain \mathbf{x}_t for all entities t . Given a set T of test triples, $2|T|$ forward passes of $Encoder_{hr}$ are required to get \mathbf{x}_{hr} for every triple $(h, r, ?) \in T$ and its inverse triple $(t, r^{-1}, ?)$, thus resulting in $O(|E| + |T|)$ computation in total.

B Markov Chain Monte Carlo Based Subgraph Sampling

Algorithm 1: MCMC-based Subgraph Sampling

Input: DFS path $D = \{t_1, t_2, \dots, t_d\}$, proposal distribution q , number k of negative samples, *burn_in* period

Output: negative tails

Initialize current negative node x at random
 $i \leftarrow 0, S \leftarrow \emptyset$

for each triple t in D **do**

- Initialize j as 0
- $h, r \leftarrow$ head, relation in triple
- if** $i \leq burn_in$ **then**

 - $i \leftarrow i + 1$
 - Sample an entity y from $q(y|x)$
 - Generate $r \in [0, 1]$ uniformly at random
 - if** $r \leq \min(1, \frac{\cos(\mathbf{x}_{hr}, \mathbf{x}_y)^\alpha}{\cos(\mathbf{x}_{hr}, \mathbf{x}_x)^\alpha} \frac{q(x|y)}{q(y|x)})$
 - then**
 - $x \leftarrow y$

- else**

 - while** $j < k$ **do**
 - Sample an entity y from $q(y|x)$
 - Add y to S
 - $x \leftarrow y$
 - $j \leftarrow j + 1$

return S ;

Inspired by a negative sampling approach (Yang et al., 2020) based on Markov chain Monte Carlo (MCMC) in a general graph, we propose a new method to sample subgraphs from a KG. A negative sampling distribution should be positively but sublinearly correlated with the positive sam-

pling distribution, which was validated by Yang et al. (2020). To include the entities close to a positive triple in the KG in negative triples, we define the sampling distribution p_n of the negative tail \hat{t} as : $p_n(\hat{t}|h, r) \propto p_d(\hat{t}|h, r)^\alpha, 0 < \alpha < 1$, $p_d(\hat{t}|h, r) = \frac{\cos(\mathbf{x}_{hr}, \mathbf{x}_{\hat{t}})}{\sum_{e \in E} \cos(\mathbf{x}_{hr}, \mathbf{x}_e)}$. where α is a parameter to stabilize the optimization process, E is a set of entities in the KG, and p_d is the sampling distribution of the positive tail. Calculating the normalization term in $p_d(\hat{t}|h, r)$ is time consuming and almost impossible. Therefore, we sample a negative tail \hat{t} from $\tilde{p}_d = \cos(\mathbf{x}_{hr}, \mathbf{x}_{\hat{t}})$ by using the Metropolis-Hastings (M-H) algorithm, and randomly select a triple whose head is \hat{t} .

Algorithm 1 describes the process of sampling a subgraph by the M-H algorithm. To prepare a mini-batch of triples for SaaM, we traverse KG using depth-first search (DFS). From each entity $e \in E$, we perform DFS until we visit d triples. For every visited triple along the DFS path, the triple inherits the probability distribution \tilde{p}_d from the previous triple in the path, and k negative tails \hat{t} are sampled from this distribution. Then \tilde{p}_d is updated. The proposal distribution q is defined as a mixture of uniform sampling and sampling from the nearest k nodes with the 0.5 probability each (Yang et al., 2020). Both d and k above are hyperparameters. The d triples in a DFS path, the sampled $d \times k$ triples, and their inverse triples compose a subgraph. We throw away the tails \hat{t} extracted during the *burn-in* period, and use the tails extracted after the period as the heads of the triples in the subgraph.

C Datasets

In this paper, we use four KGC benchmarks. WN18RR is a sparse KG with a total of 11 relations and $\sim 41k$ entities. WN18RR is the dataset derived from WN18, consisting of relations and entities from WordNet (Miller, 1992). WN18RR addresses the drawbacks of test set leakage by removing the inverse relation in WN18. NELL-995 is a sparse KG extracted from the web. FB15k-237 is a dense KG with 237 relations. Wikidata5M, a much larger KG than the others, provides transductive and inductive settings. Wikidata5M-Trans is for the transductive setting, where entities are shared and triples are disjoint across training, validation, and test. Wikidata5M-Ind is for the inductive setting, where the entities and triples are mutually disjoint across training, validation, and

WN18RR				
Size	MRR	Hits@1	Hits@3	Hits@10
512	0.591	0.571	0.604	0.713
1024	0.689	0.617	0.741	0.831
1536	0.679	0.608	0.732	0.818
2048	0.652	0.598	0.668	0.715
FB15k-237				
Size	MRR	Hits@1	Hits@3	Hits@10
1024	0.322	0.234	0.347	0.500
2048	0.339	0.250	0.368	0.521
3072	0.368	0.279	0.400	0.548
4096	0.357	0.261	0.357	0.532

Table 7: The results of investigating the model performance with respect to the batch size.

Algorithm	Sampling Time			
	WN18RR	FB15k-237	Wiki5M-Trans	Wiki5M-Ind
BRWR	13m	1h	14h	14h
Shortest Path + Degree	7m	15m	7h	7h
Training Time (SATKGC: time per phase, others: time per epoch)				
Model	WN18RR	FB15k-237	Wiki5M-Trans	Wiki5M-Ind
SATKGC	7m	30m	10h	10h
SimKGC (Wang et al., 2022a)	4m	20m	9h	9h
StAR (Wang et al., 2021a)	1h	1h 30m	-	-
SANS (Ahrabian et al., 2020)	45m	57m	-	-

Table 8: The elapsed time required for sampling and the time allotted per phase during training.

test (Wang et al., 2021c).

D Implementation Details

In our weighted InfoNCE loss, additive margin γ is set to 0.02. We select the best performing batch sizes of 1024 from 512, 1024, 1536, 2048 for WN18RR, NELL-995, and Wikidata5M, and 3072 from 1024, 2048, 3072, 4096 for FB15k-237. We set the restart probability p_r to 1/25 in BRWR. We used six A6000 GPUs and 256G RAM. Training on WN18RR took 50 phases, for a total of 4 hours. NELL-995 and FB15k-237 took 20 phases and a total of 3 hours and 10 hours respectively, while Wikidata5M took 2 phases and 20 hours.

E Runtime Analysis

Training SATKGC incurs a marginal computational overhead because (i) sampling subgraphs and (ii) computing distances and degrees are performed in advance before training. As shown in Table 8, the computational cost for (i) and (ii) is acceptable. The cost depends on the size of a mini-batch, which can be adjusted. Moreover, the time complexity for (ii) is acceptable. For each mini-batch B of triples, we run Dijkstra’s single source shortest path algo-

WN18RR				
Method	MRR	Hits@1	Hits@3	Hits@10
StAR (Wang et al., 2021a)	0.398	0.238	0.487	0.698
StAR+SaaM	0.411	0.261	0.511	0.729
FB15k-237				
Method	MRR	Hits@1	Hits@3	Hits@10
StAR (Wang et al., 2021a)	0.288	0.195	0.313	0.480
StAR+SaaM	0.319	0.220	0.334	0.490

Table 9: Performance comparison between original StAR and StAR+SaaM where StAR+SaaM stands for the StAR model architecture trained by our training framework SaaM.

rithm, and thus the runtime to compute the distance is $O(|V| \log |V| + |B| \log |V|)$, where V is a set of entities in B . As described in Section 4.3.1, we do not calculate all-pair shortest paths for every pair of vertices in V . To reduce the computational overhead, we compute the approximate distance by using the shortest path between the head of the center triple in a subgraph and every tail in that subgraph, which have been already obtained from Dijkstra’s algorithm. Table 8 shows the training time per phase for SATKGC and per epoch for SimKGC (Wang et al., 2022a), StAR (Wang et al., 2021a), and SANS (Ahrabian et al., 2020). SATKGC remains competitive, though it takes slightly more time than SimKGC due to the computational overhead for (a) computing its loss using the shortest path weight (SPW) and degree weight (DW), (b) counting the occurrences of visited triples to select the next subgraph, and (c) fetching subgraphs. StAR and SANS take longer than SATKGC. StAR runs out of memory on the Wikidata5M datasets, while SANS cannot be applied to the inductive setting (Wikidata5M-Ind), and is not expected to finish within a reasonable time on Wikidata5M-Trans.

F Effectiveness of SaaM

To demonstrate the generality of SaaM, we apply SaaM to another text-based method StAR (Wang et al., 2021a), which adopted Siamese network architecture. Table 9 shows the results where StAR+SaaM stands for the StAR model architecture trained by our training framework SaaM. Performance improvement are observed in all evaluation metrics, with significant gain in MRR and Hits@1. These results empirically validate that the model-agnostic SaaM framework can be successfully applied to different text-based methods.

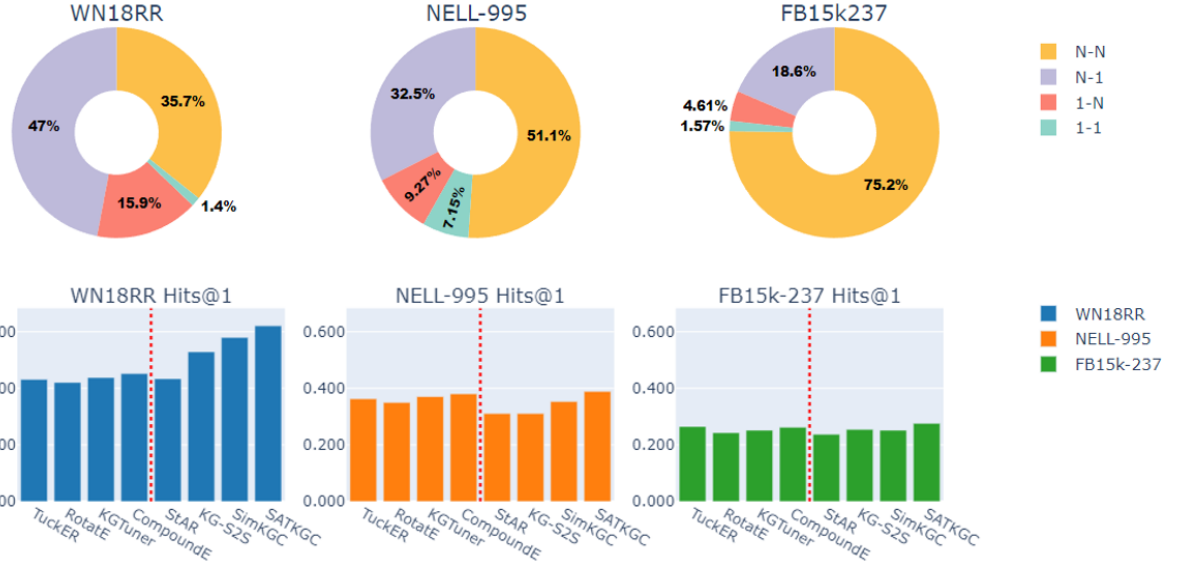


Figure 7: The ratio of triples categorized by relation type for the WN18RR, NELL-995, and FB15k-237 datasets, along with the corresponding Hits@1 performance results for each dataset.

WN18RR				
Method	MRR	Hits@1	Hits@3	Hits@10
Mixed	0.665	0.586	0.722	0.814
SaaM	0.689	0.621	0.731	0.823
FB15k-237				
Method	MRR	Hits@1	Hits@3	Hits@10
Mixed	0.346	0.249	0.388	0.534
SaaM	0.368	0.276	0.401	0.548

Table 10: Performance comparison between Mixed and SaaM, where Mixed replaces half of in-batch triples generated by BRWR with randomly selected triples.

G Performance of Hybrid In-Batch Negatives

To evaluate the efficacy of constructing a batch exclusively with triples in a subgraph (i.e., SaaM), we compare two sampling methods SaaM and Mixed. Mixed represents a variant that replaces a half of triples in each mini-batch produced by SaaM with randomly selected triples. Table 10 illustrates the performance of SaaM and Mixed. Including random samples deteriorates performances, e.g., a significant drop in Hits@1, which indicates that a mini-batch consisting only of triples within the subgraph is more beneficial.

H False Positive Analysis

We aim to demonstrate that our contrastive learning with two structure-aware factors selectively pe-

Triples	$\psi_h L_{(h,r,t)}$	$L_{(h,r,t)}$
total triples	0.2268	0.1571
false positives	0.4987	0.2834

Table 11: Comparison of average loss values on WN18RR for total triples and false positives in the batch.

nalizes hard negative triples. Table 11 compares $\psi_h L_{(h,r,t)}$ and $L_{(h,r,t)}$ on average only for false positives and those for all training triples, where $L_{(h,r,t)}$ in Equation (1) represents loss with only the distance factor ω_{ht_i} applied, and $\psi_h L_{(h,r,t)}$ in Equation (2) additionally applies the degree factor ψ_h . The average loss values for the false positives are higher than those for all the triples, which indicates that the structure-aware contrastive learning method severely punishes incorrect predictions for hard negative triples.

I Correlation of Relation Types and Performances

We investigate the distribution of triples based on their relation types on WN18RR, NELL-995, and FB15k-237. Figure 7 shows that the ratio of triples with the N-N relation type increases in the order of WN18RR, NELL-995, and FB15k-237, while the ratio of triples with the N-1 and 1-N relation types decreases in the same order. In Table 2, both embedding-based and text-based approaches achieve the best results on WN18RR among the

Approach	WN18RR				NELL-995				FB15k-237			
	MRR	Hits@1	Hits@3	Hits@10	MRR	Hits@1	Hits@3	Hits@10	MRR	Hits@1	Hits@3	Hits@10
<i>Embedding-based approach</i>												
SANS (Ahrabian et al., 2020)	0.216	0.027	0.322	0.509	0.359	0.309	0.381	0.493	0.298	0.203	0.331	0.486
TransE (Bordes et al., 2013)	0.239	0.421	0.450	0.510	0.383	0.321	0.400	0.492	0.280	0.193	0.372	0.439
DistMult (Yang et al., 2015)	0.435	0.410	0.450	0.510	0.409	0.343	0.427	0.515	0.280	0.195	0.297	0.441
TuckER (Balazevic et al., 2019)	0.466	0.432	0.478	0.518	0.423	0.363	0.455	0.536	0.361	0.265	0.391	0.538
RotatE (Sun et al., 2019)	0.471	0.421	0.490	0.568	0.411	0.350	0.439	0.522	0.335	0.243	0.374	0.529
KG Tuner (Zhang et al., 2022)	0.481	0.438	0.499	0.556	0.428	0.371	0.458	0.544	0.345	0.252	0.381	0.534
CompoundE (Ge et al., 2023)	0.492	0.452	0.510	0.570	0.434	<u>0.381</u>	0.466	0.550	0.350	0.262	0.390	0.547
CSProm-KG (Chen et al., 2023)	0.569	0.520	0.590	0.675	0.422	<u>0.381</u>	<u>0.474</u>	0.535	0.355	0.261	0.389	0.531
<i>Text-based approach</i>												
KG-BERT (Yao et al., 2019)	0.216	0.040	0.298	0.516	0.199	0.021	0.267	0.488	0.158	0.019	0.232	0.420
MTL-KGC (Kim et al., 2020)	0.331	0.203	0.383	0.597	0.288	0.176	0.229	0.411	0.267	0.172	0.298	0.458
StAR (Wang et al., 2021a)	0.398	0.238	0.487	0.698	0.419	0.238	0.395	0.433	0.288	0.195	0.313	0.480
HaSa (Zhang et al., 2023a)	0.538	0.444	0.588	0.713	0.411	0.310	0.431	0.524	0.304	0.220	0.325	0.483
KG-S2S (Chen et al., 2022)	0.572	0.529	0.595	0.663	0.416	0.311	0.421	0.519	0.337	0.255	0.374	0.496
SimKGC (Wang et al., 2022a)	0.671	0.580	0.729	0.811	0.425	0.353	0.447	0.531	0.340	0.252	0.365	0.515
GHN (Qiao et al., 2023) [†]	0.678	0.596	0.719	<u>0.821</u>	-	-	-	-	0.339	0.251	0.364	0.518
<i>Ensemble approach</i>												
StAR(Ensemble) (Wang et al., 2021a)	0.520	0.456	0.509	0.707	0.415	0.311	0.402	0.510	0.332	0.229	0.387	0.526
SATKGC-SPW-DW	0.672	0.605	0.714	0.811	0.411	0.310	0.431	0.524	0.304	0.220	0.325	0.483
SATKGC-DW	0.679	0.609	0.723	0.813	0.429	0.361	0.466	0.551	0.351	0.261	0.372	0.525
SATKGC-SPW	<u>0.681</u>	<u>0.612</u>	<u>0.729</u>	<u>0.820</u>	0.431	0.369	0.472	<u>0.556</u>	0.359	<u>0.271</u>	<u>0.393</u>	0.538
SATKGC	0.689	0.621	0.731	0.823	<u>0.433</u>	0.389	0.476	0.560	0.368	<u>0.276</u>	0.401	0.548

Table 12: KGC results for the WN18RR, NELL-995, and FB15k-237 datasets. “SPW” and “DW” refer to shortest path weight and degree weight respectively. The best and second-best performances are denoted in **bold** and underlined respectively. [†]: numbers are from Qiao et al. (2023).

three datasets, whereas the performance is worse on FB15k-237. We observe that a high proportion of the N-N relation type and a low proportion of the N-1 and 1-N relation types negatively impact the model performance.

This performance difference between the datasets is larger for a text-based approach than for an embedding-based approach. We speculate that this is because the embedding-based approach randomly initializes the entity and relation embeddings, while the text-based approach uses contextualized text embeddings obtained from PLMs. For the N-N relations where multiple tails can be the correct answer for the same (h, r) pair, the embeddings of these correct tails should be similar. However, PLMs take only text as input, being oblivious of their high similarity. Therefore, these tail embeddings generated by the PLMs might be far apart from each other, so the (h, r) embedding is likely to remain in the middle of these tail embeddings during fine-tuning.

J Hyperparameter Sensitivity

We investigate how restart probability p_r in BRWR affects model performance. The hyperparameter p_r is associated with the length of the random walk path from the start entity, which in turn influences the occurrence of duplicate entities in a mini-batch. A longer path leads to fewer duplicate entities in the mini-batch. Figure 8(a) illustrates that a lower p_r value, encouraging a longer random walk path,

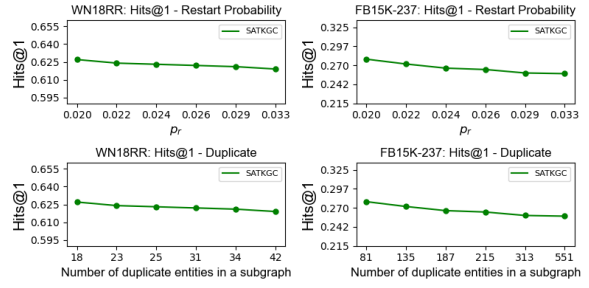


Figure 8: (a) Impact of varying restart probabilities on the model performance. (b) Impact of varying the number of duplicate entities in a mini-batch on the model performance.

leads to higher Hits@1 for WN18RR and FB15k-237. We analyze the impact of duplicate entities in a mini-batch on the model performance. In Figure 8(b), more duplicate entities resulting from higher p_r negatively impact on the performance, which highlights the importance of reducing the duplicates in a mini-batch to avoid the performance degradation.

K Entire Main Results

Table 12 presents the results of all baselines compared with ours.